

Application of a novel gelled-electrolyte in valve-regulated lead-acid batteries with tubular positive plates

Zheng Tang · Jian-Ming Wang · Xian-Xian Mao ·
Quan-Qi Chen · Chen Shen · Jian-Qing Zhang

Received: 8 January 2007 / Revised: 12 July 2007 / Accepted: 16 July 2007 / Published online: 3 August 2007
© Springer Science+Business Media B.V. 2007

Abstract A polysiloxane-based gel electrolyte (PBGE) was prepared and used as a novel gel electrolyte in valve-regulated lead-acid (VRLA) batteries with tubular positive plates. Cyclic voltammetry (CV) and scanning electron microscopy (SEM) indicated that PBGE is more stable than fumed-silica gel electrolyte (FSGE). The properties of AGM (absorptive glass mat)-PBGE and PVC-FSGE tubular batteries were investigated by electrochemical techniques. The results showed that the AGM-PBGE tubular batteries have higher initial discharge capacity and better high-low temperature performance than PVC-FSGE. The improved electrochemical performance of the AGM-PBGE batteries may result from the high charge efficiency and the open three-dimensional network structure of PBGE. SEM and X-ray diffraction (XRD) spectroscopy showed that PBGE facilitates the conversion of the active-mass to lead dioxide, presenting a high formation efficiency. The addition of PBGE instead of FSGE not only simplifies the manufacturing process of tubular gel batteries, but also improves the utilization efficiency of positive active material (PAM), thus enhancing the battery performance and reducing the manufacturing cost.

Keywords Polysiloxane-based gel electrolyte · Fumed silica gel electrolyte · Tubular positive plates · Positive active material · Valve-regulated lead-acid (VRLA) batteries

1 Introduction

The main problems for AGM-VRLA batteries include softening or shedding of PAM, thermal runaway and premature capacity loss (PCL). A gel battery is a good substitute for an AGM battery because it may alleviate or prevent problems encountered in conventional AGM batteries such as drainage, electrolyte stratification, sulphation, thermal runaway, PCL and micro short-circuit due to dendrites. However, softening and shedding of PAM in flat plates remain causes for gel battery failure. Since softening and shedding of the active materials in tubular positive plates can be alleviated or prevented, lead-acid batteries with tubular positive plates may present flatter discharge curves, longer cycle life and larger capacity than those with flat plates [1–6]. It is expected that gel batteries with tubular positive plates can display excellent performance.

The manufacturing process of conventional gel batteries with tubular positive plates (PVC-FSGE tubular batteries) is very complex and battery performance needs to be further improved [7, 8]. In order to simplify the manufacturing process of the tubular gel batteries and improve their properties, colloid gel instead of acid was directly filled into the hybrid batteries in which AGM separator and gel electrolyte were integrated [8–10]. However, the conversion of the active-mass to the desired lead dioxide is unsatisfactory because of fast gelling and poor penetration of reactive species into the thick tubular positive plates (8.5–9.8 mm). A necessary way of aiding the formation

Z. Tang · J.-M. Wang (✉) · Q.-Q. Chen · C. Shen ·
J.-Q. Zhang
Department of Chemistry, Zhejiang University, Hangzhou
310027, P.R. China
e-mail: wjm@zju.edu.cn

X.-X. Mao
Zhejiang Narada Power Source Co., Ltd, Hangzhou 310013,
P.R. China

J.-Q. Zhang
Chinese State Key Laboratory for Corrosion and Protection,
Shenyang 110015, P.R. China

process of the active mass is continuous addition of red lead (Pb_3O_4) to the oxide (PbO) during the tube filling process [11, 12], but high content of red lead is detrimental to uniform distribution of composite phase and compact bonding between the particles of active materials [11]. Moreover, the manufacturing cost of the present tubular gel batteries is relatively high. Therefore, a novel electrolyte with a simple manufacturing process is imperative.

Polysiloxane compounds, one kind of polymer with Si–O bonds in their main chains, are widely used as solid polymer electrolyte in electrochemical systems (e.g. lithium polymer batteries) due to their high ionic conductivity, good thermal, chemical and mechanical stabilities as well as excellent flexibility [13–15]. Recently, a novel application of PBGE in lead-acid batteries with pasted positive plates has been reported [16]. In the present work a mixed polysiloxane gel is used as a new gelling agent in VRLA tubular batteries. The electrochemical properties and manufacturing process of the AGM-PBGE tubular batteries are investigated and compared with those of the PVC-FSGE ones.

2 Experimental

2.1 Preparation of gelled-electrolyte

2.1.1 Preparation of fumed silica electrolyte (raw gel)

Aerosil 200 (A200) fumed silica (supplied by Degussa Corp.) was used to prepare raw gel. A200 fumed silica was dispersed and diluted in water with a pH range of 4.1–4.7; thus a suspension solution was obtained. Sodium sulfate and phosphoric acid as additives were added to the suspension solution and their concentrations were 5.5 and 55 g L^{-1} , respectively. The details of preparation procedure were described elsewhere [17].

2.1.2 Preparation of polysiloxane-based gel electrolyte (PBGE)

The mixed polysiloxane gel was prepared by the following procedure. Appropriate amounts of poly-ether modified siloxane with hydrophilic group (molecular weight < 3,000), methyl silicon oil (viscosity < 1500P), tetraethyloxysilane (TEOS) and deionized water were mixed and strongly stirred. The detailed synthesis procedure had been previously described [16, 18, 19]. PBGE was prepared by mixing the above obtained polysiloxane gel, deionized water and sulphuric acid (1.53 g cm^{-3}) at a weight ratio of 1:4.9:6.0. The calculated content of H_2SO_4 in PBGE was nearly identical with that in normal tubular batteries [20].

2.2 Electrochemical tests

Cyclic voltammetry was carried out in a classical three-electrode cell using a model 273A potentiostat/galvanostat, with a scanning rate of 10 mV s^{-1} . A planar lead alloy (0.9%Sn–0.09%Ca) electrode with an exposed geometric area of 1 cm^2 was used as working electrode. A platinum foil was employed as counter electrode and a $\text{Hg}/\text{Hg}_2\text{SO}_4$ electrode as reference.

2.3 Assembly of two tubular gel batteries

2.3.1 Preparation of traditional tubular positive plates and flat negative plates

After the spines of Pb–Ca–Sn alloy had been inserted into non-woven porous polymer tubes, the mixture of grey oxide and red lead with a weight ratio of 3:1 was filled into the tubes. The filled tubular plates were dipped in sulphuric acid with a density of 1.15 g cm^{-3} for 10 min; then the dipped plates were washed with deionized water to remove any excess acid and were air-dried in a chamber set at 45–50 °C and 20–35% humidity for 24 h. The manufacturing process of flat negative plates for the two gel batteries is the same as that for normal AGM batteries.

2.3.2 Assembly and formation of two tubular gel batteries

The two tubular gel batteries rated as 2 V/200 Ah were assembled using the same technology and components except for different electrolytes and separators. AGM and PVC separators were used in AGM-PBGE and PVC-FSGE tubular batteries, respectively. In order to improve the even distribution of electrolyte between plates and separator, PBGE was filled into battery cases using a vacuum system, and the filled AGM-PBGE tubular batteries were allowed to rest for several hours in open-circuit state before formation. The formation algorithm was almost the same as that of normal AGM batteries. The formation of conventional PVC-FSGE tubular batteries was firstly conducted in a lower density acid, and the second stage of formation was carried out in the sulphuric acid solution of density 1.26 g cm^{-3} . After the formed batteries had been discharged to 150% of nominal capacity at different current densities, the residual electrolyte was replaced by the prepared raw gel. The filled FSGE began to gradually solidify when sulphuric acid was released from the plates due to PbSO_4 oxidation into PbO_2 at the positive plates and PbSO_4 reduction into Pb at the negative plates during the next charge steps. The formation of PVC-FSGE tubular batteries was carried out using a common, multi-step charge–discharge algorithm. The details of formation algorithms for the two tubular gel batteries are presented in Tables 1 and 2.

Table 1 Formation algorithm for AGM-PBGE tubular batteries

| Step | Program | Current (A) | Voltage (V) | Time (h) |
|------|-----------|---------------------------------|-------------|-------------|
| 1 | Rest | – | – | 2 |
| 2 | Charge | 0.5I ₁₀ ^a | – | 20 |
| 3 | Charge | I ₁₀ | – | 32 |
| 4 | Discharge | I ₁₀ | – | 0.5 |
| 5 | Charge | I ₁₀ | – | 30 |
| 6 | Discharge | I ₁₀ | – | 0.5 |
| 7 | Charge | 0.5 I ₁₀ | – | 30 |
| 8 | Discharge | I ₁₀ | 1.8 | 10–12 |
| 9 | Charge | I ₁₀ | 2.5 | ~12 |
| 10 | Charge | 0.5 I ₁₀ | 2.5 | 10 |
| 11 | Discharge | 0.5 I ₁₀ | – | 0.5 |
| 12 | Charge | 0.5 I ₁₀ | 2.5 | 15 |
| 13 | Charge | 0.5 I ₁₀ | | 5 |
| 14 | Charge | 0.1 I ₁₀ | 2.23 | 5 |
| 15 | Total | | | About 175 h |

^a I₁₀=0.1C₁₀

2.4 Battery test

The high-rate discharge tests for the AGM-PBGE and PVC-FSGE tubular batteries (2 V/200 Ah) were performed with Digatron UBT series instruments. The high-low temperature and cycle-life tests of the two tubular batteries (100% DOD-depth of discharge) were conducted using Bitrode battery test modules and an Arbin BT-2000 system, respectively. The tests of oxygen-recombination rate and internal resistance were carried out according to IEC (International Electrotechnical Commission) 60896-2-1 standard.

2.5 Physical characterization

The morphologies of the samples were observed by scanning electron microscopy (SEM) with a SIRION-100 microscope (FEI, USA). The crystal structures of the samples were determined by X-ray diffraction (XRD) analysis using a Rigaku D/Max 2550 X-ray diffractometer

Table 2 Formation algorithm for PVC-FSGE tubular batteries

| Step | Program | Current (A) | Voltage (V) | Time (h) | Remarks |
|------|--|---------------------|-------------|-------------|---|
| 1 | Rest | – | – | 2 | Acid density: 1.10 g cm ⁻³ (20 °C) |
| 2 | Charge | 1.4I ₁₀ | – | 24 | |
| 3 | Charge | 0.6 I ₁₀ | – | 20 | |
| 4 | Rest | 0.2 I ₁₀ | – | 5 | Acid density: 1.24 g cm ⁻³ (20 °C) |
| 5 | Discharge | 2 I ₁₀ | 1.8 | ~5 | |
| 6 | Charge | 2 I ₁₀ | 2.4 | ~5 | |
| 7 | Charge | 0.5 I ₁₀ | | 20 | |
| 8 | Continuing 2 cycle from step 5 to step 7 | – | – | ~60 | |
| 9 | Adjusting acid | 0.2 I ₁₀ | | ~5 | Acid density: 1.26 g cm ⁻³ (20 °C) |
| 10 | Continuous discharge | | | ~24 | Discharged to 150% nominal capacity |
| 11 | Rest | | | 2 | Removing free acid and filling raw gel |
| 12 | Charge | 1.4I ₁₀ | 2.3 | ~6 | Gelling and formation |
| 13 | Charge | 0.6 I ₁₀ | | 8 | |
| 14 | Charge | 0.3 I ₁₀ | | 7 | |
| 15 | Discharge | 1.72I ₁₀ | | 5 | |
| 16 | Charge | 1.4 I ₁₀ | 2.4 | ~7 | |
| 17 | Charge | 0.6 I ₁₀ | | 8 | |
| 18 | Charge | 0.3 I ₁₀ | | 7 | |
| 19 | Discharge | I ₁₀ | 1.8 | ~10 | |
| 20 | Charge | I ₁₀ | 2.4 | 20 | |
| 21 | Total | | | About 250 h | |

with Cu K α radiation at 40 kV and 300 mA, and a scanning rate of 8° (2 θ)/min.

3 Results and discussion

3.1 The properties of gel electrolytes

Figure 1 presents the cyclic voltammograms (CV) of the planar lead alloy electrode in PBGE and sulphuric acid systems. The two CV curves show similar redox peaks in the potential range -1.4 V– 1.4 V, suggesting that the redox processes of lead are not altered by the addition of polysiloxane-based polymer in sulphuric acid electrolyte. More positive oxygen evolution potential, more negative hydrogen evolution potential and the corresponding lower peak currents imply that hydrogen and oxygen evolution reactions are inhibited in the PBGE system. This is advantageous to improving battery performance. The CV also indicates that polysiloxane-based polymer is stable under the operating conditions of VRLA batteries.

Figs. 2(a) [16] and 3(a) show the SEM micrographs of the prepared polysiloxane sample and fumed silica electrolyte, respectively. It can be seen from Fig. 2(a) that the polysiloxane sample displays uniform spherical particles with a size of 30–50 nm. Little agglomeration or crosslinking of the polysiloxane particles after storage for one month indicates their excellent dispersion and stability. Figure 3 (a) shows that some aggregations of fumed silica occur after storage. Accordingly, it is required in battery factories that the prepared raw gel of fumed silica should be filled into battery cases on the same day. Figs. 2(b) and 3(b) show the SEM images of polysiloxane-based gel electrolyte (PBGE) and fumed-silica gel electrolyte (FSGE) with sulphuric acid after storage for one month,

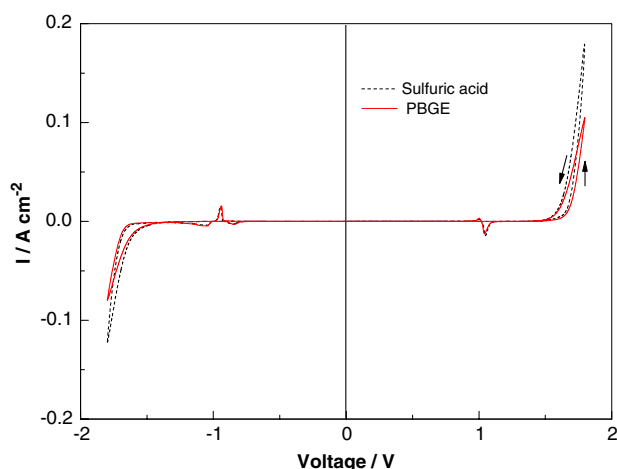


Fig. 1 Cyclic voltammogram curves of lead alloy in PBGE and sulphuric acid in the potential range of -1.8 V– 1.8 V at 10 mV s $^{-1}$

respectively. A three-dimensional network structure formed by inter-particle or intra-particle crosslinking in the acid medium can be clearly observed in Fig. 2(b). Blurred aggregations are observed in Fig. 3(b) because of the gelling and agglomeration of fumed silica with sulphuric acid. The large aggregations in FSGE may lead to poor contact between gel, plates and separators.

Figure 4(a) and (b) show the SEM images of PBGE in the AGM separator in charged and discharged states, respectively. The particle sizes of PBGE in Fig. 2 (a) and (b) are smaller than those in Fig. 4 (a) and (b), respectively. The former has begun to swell after storage for one month [21] due to the absence of charge, discharge or shear strains, while the latter exhibits good thixotropic properties during cyclic operation. The full formation in charged state (Fig. 4a) and partial disruption in discharged state (Fig. 4b) of the three-dimensional network framework of the gel electrolyte mainly results from changes in sulphuric acid concentration and charge quantity. This may play an important role in improving oxygen-recombination rate and charge-discharge efficiency due to the reversible conversion of sol and gel states.

In our work, the oxygen-recombination rate of the PVC-FSGE tubular batteries is 95.0%, obviously lower than that (99.2%) of the AGM-PBGE tubular batteries in the initial period. This is because the formation of the cracks in normal gel electrolyte, which is necessary for oxygen diffusion from positive plates to negative ones, needs some time [8]. After the raw gel is filled into the PVC-FSGE tubular batteries, the short formation time and precycling makes it more difficult for micro or macro-cracks to be formed during battery formation. However, the oxygen-recombination rate of the AGM-PBGE tubular batteries is almost the same as that of AGM batteries [22]. This suggests that the gel structure with polysiloxane-based polymer may facilitate the formation of micropores in the AGM separator. Therefore, higher charge efficiency, lower water loss or better charge acceptance for AGM-PBGE tubular batteries can be expected during initial cycles.

3.2 Battery performance

The internal resistance of the AGM-PBGE and PVC-FSGE tubular batteries (2 V/200 Ah) is determined to be 0.726 and 0.939 m Ω , respectively. Figures 5 and 6 show that the AGM-PBGE tubular batteries present higher discharge voltage and larger high-rate discharge capacity than PVC-FSGE. The micropores in PBGE may provide a pathway for the diffusion of reactive species such as H $_2$ O and H $_2$ SO $_4$, hence the concentration polarization during charge and discharge is reduced by enhancing the transfer

Fig. 2 SEM images of polysiloxane-based polymer before (a) and after (b) gelling with sulphuric acid (1.285 g cm⁻³) (storage for one month)

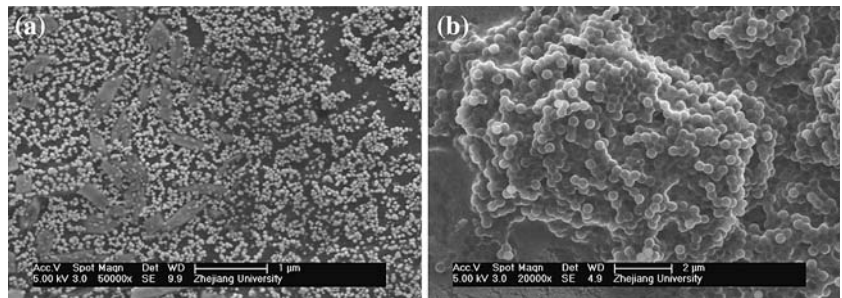


Fig. 3 SEM images of fumed-silica electrolyte before (a) and after (b) gelling with sulphuric acid (1.285 g cm⁻³) (storage for one month)

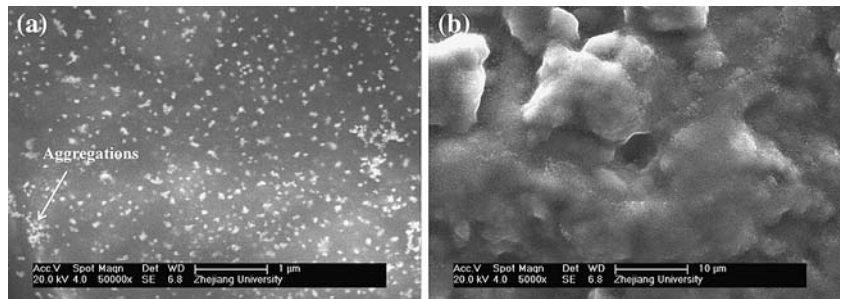


Fig. 4 SEM images of polysiloxane-based gel electrolyte in the charged (a) and discharged (b) states in the AGM separators

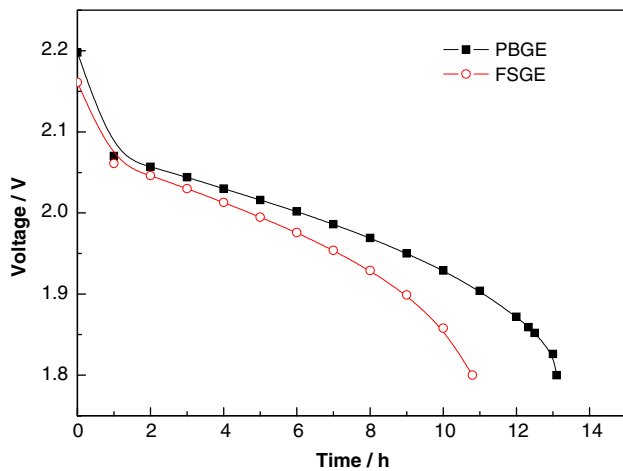
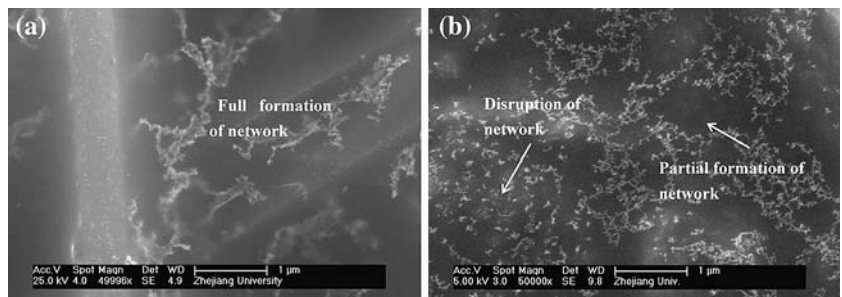


Fig. 5 Initial discharge curves for the AGM-PBGE and PVC-FSGE tubular batteries (2 V/200 Ah) at 10 h rate

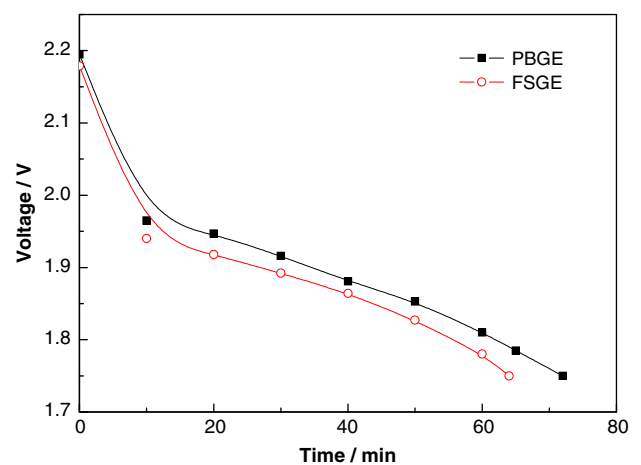


Fig. 6 Initial discharge curves for the AGM-PBGE and PVC-FSGE tubular batteries (2 V/200 Ah) at 1 h rate

of reactive species between positive and negative plates [16]. This may be partially responsible for the lower internal resistance and better discharge performance of the AGM-PBGE batteries.

Figure 7 shows the low-temperature discharge performance of the two tubular batteries (2 V/200 Ah) fully charged at 0.1 C rate for 24 h. The AGM-PBGE tubular batteries display higher discharge voltage and much longer discharge time than PVC-FSGE at $-10\text{ }^{\circ}\text{C}$. The discharge capacity of AGM-PBGE tubular batteries at $55\text{ }^{\circ}\text{C}$ is 25% higher than that of PVC-FSGE (The related data are not shown).

Figure 8 shows the cyclic performance of the two tubular batteries. The AGM-PBGE tubular batteries present much larger discharge capacity than PVC-FSGE in all the 50 cycles. This results from the higher formation efficiency and utilization of PAM in PBGE plates. It can be seen that the discharge capacities of the two tubular batteries gradually increase in the initial cycles. The gradual formation of cracks induces an increase in oxygen-recombination rate; thus higher charge efficiency is obtained.

Figure 9 shows SEM micrographs of the fully charged PAM in the newly formed AGM-PBGE and PVC-FSGE tubular batteries. The initial PAM in the AGM-PBGE tubular batteries displays much smaller grain size and more porous structure than that in PVC-FSGE, as a result of the formation of an open three-dimensional network framework due to the rapid penetration of polysiloxane-based particles in the plates. The formation of a strong and open skeleton is beneficial for improving the access of reactive species such as H_2O and H_2SO_4 to the interior PAM of PBGE plates. This is one of main reasons for the enhanced utilization of PAM and improved high-rate discharge performance in the PBGE system.

Chemical analysis results show that the content of PbO_2 in the fully charged PAMs of the newly formed AGM-

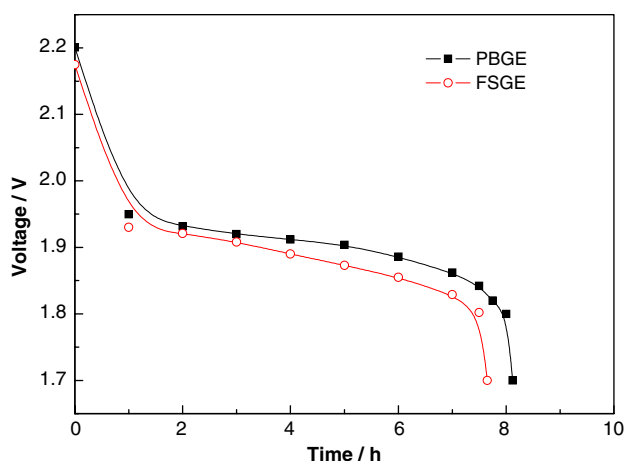


Fig. 7 Discharge performance of the AGM-PBGE and PVC-FSGE tubular batteries (2 V/200 Ah) at $-10\text{ }^{\circ}\text{C}$ and 10 h rate

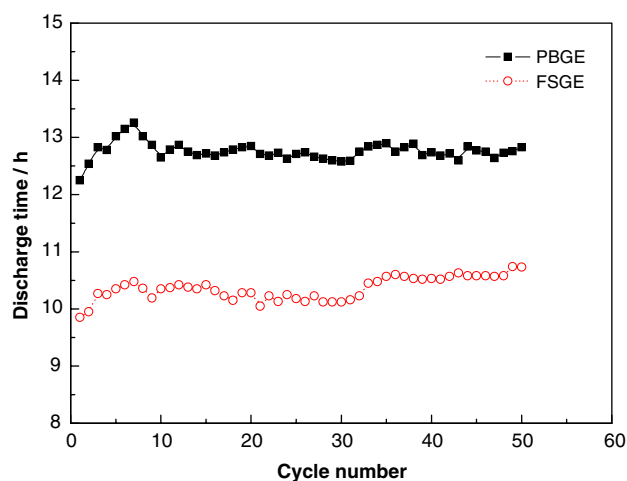


Fig. 8 Cyclic performance of the AGM-PBGE and PVC-FSGE tubular batteries (2 V/200 Ah) at $25\text{ }^{\circ}\text{C}$ and 10 h rate

PBGE and PVC-FSGE tubular batteries is 92% and 75%, respectively. This indicates that the AGM-PBGE batteries have higher formation efficiency than PVC-FSGE. Figure 10 presents the XRD patterns of PAMs in the newly formed AGM-PBGE and PVC-FSGE batteries. PbSO_4 is found in the PAM of the formed PVC-FSGE batteries, but is absent in the PAM of the formed AGM-PBGE ones, implying that PBGE instead of FSGE facilitates the conversion of the active-mass to lead dioxide. This may result from the good penetration performance and open three-dimensional network structure of PBGE.

3.3 Comparison of manufacture process for the two tubular gel batteries

Polysiloxane-based gel electrolyte can be easily prepared by mixing several composites with a high-speed mixer. The PBGE obtained has good fluidity, low viscosity and a long gel time (more than 3 h); it can even be filled into batteries without a vacuum filler. A significant reduction in formation time from 250 h for the PVC-FSGE tubular batteries to 175 h for AGM-PBGE is advantageous in reducing power cost and water loss. Moreover, the PVC-FSGE tubular batteries with lower initial capacity need to be precycled before leaving the factory, but this procedure is not necessary for the AGM-PBGE batteries, indicating that the latter needs less manufacturing time and, thus involves lower cost.

4 Conclusions

Polysiloxane-based polymer is stable under the operating condition of VRLA batteries, and its addition in the elec-

Fig. 9 SEM images of the fully charged PAMs in the newly formed AGM-PBGE (a) and PVC-FSGE (b) tubular batteries

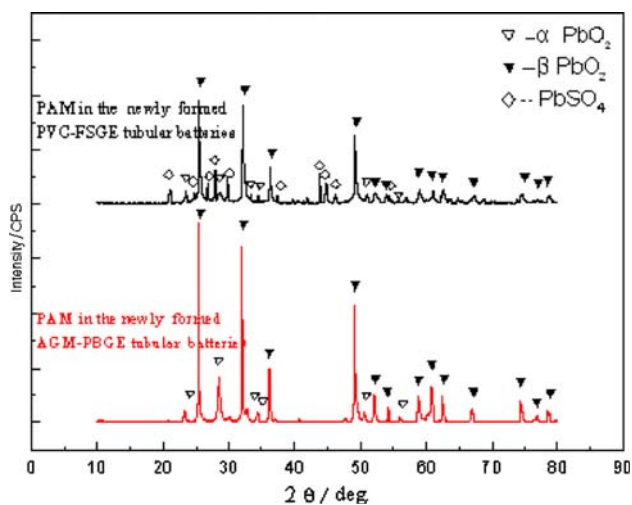
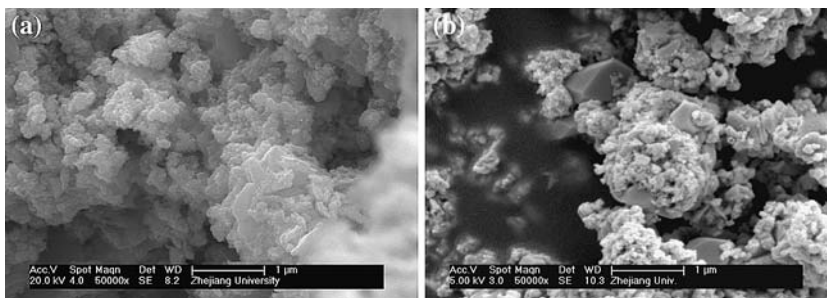


Fig. 10 XRD patterns of the fully charged PAMs in the newly formed AGM-PBGE and PVC-FSGE tubular batteries

trollyte inhibits hydrogen and oxygen evolution reactions. Compared with PVC-FSGE tubular batteries, the AGM-PBGE ones not only present superior initial performance such as high-rate discharge, high-low temperature properties and oxygen-recombination rate, but also have a shorter manufacturing time and lower cost. Improvement of the performance of AGM-PBGE tubular batteries mainly results from the high formation efficiency and enhanced utilization of PAM in PBGE plates, as well as the open three-dimensional network framework of the polymer gel electrolyte. The improved performance and simplified manufacturing process may make AGM-PBGE tubular batteries promising for industrial applications.

Acknowledgements This work was supported by R&D centre of Zhejiang Narada Power Source Co., Ltd. The authors also gratefully acknowledge financial support of the Chinese State Key Laboratory for Corrosion and Protection.

References

1. Dyson I, Griffin P (2003) *J Power Sources* 116:263
2. D’Alkaine CV, Impinisi RP, Carubelli A (2003) *J Power Sources* 113:293
3. Pavlov D, Papazov G, Monahov B (2003) *J Power Sources* 113:255
4. Guo YL, Li WZ, Zhao L (2003) *J Power Sources* 116:193
5. Guo YL, Garche J (2005) *J Electrochem Soc* 152:628
6. Prengaman RD (1995) *J Power Sources* 53:207
7. Toniazzo V (2006) *J Power Sources* 158:1124
8. Culpin B (2005) US Patent Pub. No: US2005181284
9. Martha SK, Hariprakash B, Gaffoor SA, Ambalavanan S, Shukla AK (2005) *J Power Sources* 114:560
10. Gerner SD (1994) US Patent 5376479
11. Ferg EE, Loyson P, Poorun A (2006) *J Power Sources* 155:428
12. Pavlov D, Kapkov N (1990) *J Electrochem Soc* 137:16
13. Lee II, Song GS, Lee WS, Suh DH (2003) *J Power Sources* 114:320
14. Kang Y, Lee J, Suh DH, Lee C (2005) *J Power Sources* 146:3910
15. Nakahara H, Yoon S, Nutt S (2006) *J Power Sources* 158:600
16. Tang Z, Wang JM, Mao XX, Shao HB, Chen QQ, Xu ZH, Zhang JQ (2006) Investigation and application of polysiloxane-based gel electrolyte in valve-regulated lead-acid batteries, proceedings of 10th European Lead Battery Conference, Athens, Greece, 26–29 September
17. Jache O, Schroeder H (1983) US Patent 4414302
18. Dong SQ, Nie CS (2004) CN Patent 1663984A
19. Liu YR, Feng YS (2002) CN Patent 1312331A
20. Kuhn AT, Stevenson JM (1983) *J Power Sources* 10:389
21. Linder C, Nemas M, Perry M, Katrarro R (1993) US Patent 5265734
22. Tang Z, Mao XX, Wang Y (2006) *Chinese J Power Sources* 30(3):231